Leading Edge of a Shock-Induced Boundary Layer

MARTIN SICHEL
University of Michigan, Ann Arbor, Michigan
(Received January 11, 1962; revised manuscript received May 4, 1962)

The boundary layer which is formed as a shock wave propagates down a shock tube causes both shock attenuation and shock curvature. Hartunian studied the curvature effect; however, as he points out, because of the singularities at the leading edge of the boundary layer his solution is not valid where the shock wave touches the tube wall. A detailed study is now made of the flow near the leading edge of this shock-induced boundary layer for a weak shock wave. The leading-edge flow can be divided into a shear layer near the wall, and into a free stream or shock region. By expanding the Navier–Stokes equations in the small parameter $M_1^* - 1$ and stretching the coordinates, simplified equations for the shear layer and shock region are obtained. The shear layer and shock region flows interact and it is found that the shock region must be a zone of non-Hugoniot flow where the shock structure is two dimensional. An approximate solution of the shock shape is obtained by replacing the shock region by an oblique shock which is approximately matched to the shear layer.

I. INTRODUCTION

THE extensive use of the shock tube as a research tool in high-speed aerodynamics has prompted many studies of the boundary layer formed behind a shock wave propagating down a shock tube, for this boundary layer causes both shock attenuation and shock-wave curvature.[1,2] In most investigations the main concern has been attenuation, and the influence of the boundary-layer flow upon shock shape has been neglected since schlieren pictures indicated that the shock remains plane and normal to the tube axis. The recent interest in high-altitude aerodynamics has led to shock-tube experiments with very low initial pressures and densities, and under these circumstances the measurements of Duff and Young[3] and of Lin and Fyfe[4] indicate that the shock-wave curvature caused by the boundary layer is no longer negligible. Thus the shock wave may appear as in Fig. 1(a). This curvature may cause nonuniformities in the flow behind the shock wave, and also will affect measurements of shock-wave structure.

Hartunian[5] appears to be the only one to have investigated the influence of the boundary layer upon the shock shape theoretically. He treated the two-dimensional problem of a shock wave moving past a stationary flat plate. The key assumption in his analysis is that the boundary layer only causes small perturbations in the shape of the shock wave. Thus the boundary-layer flow is computed by treating the shock as a plane discontinuity with Hugoniot conditions across it and by placing the leading edge of the boundary layer where the shock touches the wall. There are two inconsistencies in this analysis. First, the boundary-layer approximation fails near the leading edge and, of course, the solution of the boundary-layer equations is singular there. Second, if the no-slip boundary condition is valid at the plate, the shock wave or shock layer, within which there is a jump in the velocity, cannot extend undisturbed to the wall. These inconsistencies are reflected in the results of Hartunian's analysis in that the shock is tangent to the plate right at the boundary-layer leading edge and has a radius of curvature which is of the same order as the shock thickness, and Hartunian suggests that this leading-edge flow be investigated in greater detail. To develop a theory for the shock curvature which is consistent, it thus appears necessary to anandon the boundary-layer approximation near the base of the shock and to take into account the detailed interaction between the shock structure and the leading-edge flow rather than treating the shock as a mathematical discontinuity which extends to the wall.

A study of the flow near this shock-induced leading edge, where there must be a transition from the undisturbed flow ahead of the shock to the fully developed laminar boundary layer behind the shock, forms the subject of the present paper. In the analysis, a coordinate system fixed to the shock wave is used as shown in Fig. 1(b). In these co-

[1] E. Becker, Z. Flugwissenschaften 7, 61 (1959).
[2] R. J. Emrich and D. B. Wheeler, Phys. Fluids 1, 14 (1958).
[3] R. E. Duff, and J. L. Young, III, Phys. Fluids 4, 812 (1961).
[4] S. C. Lin and W. I. Fyfe, Phys. Fluids 4, 238 (1961).
[5] R. A. Hartunian, Phys. Fluids 4, 1059 (1961).

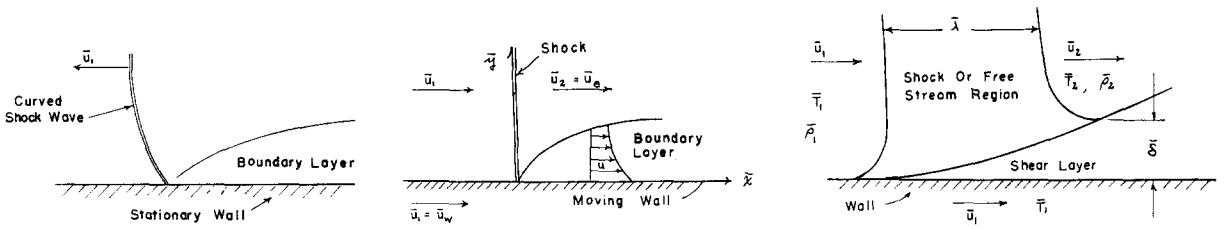

FIG. 1. (a) Boundary-layer induced curvature in a shock wave moving past the wall of a shock tube; (b) Shock wave moving past a stationary flat plate as seen from a coordinate system fixed to the shock wave; (c) Theoretical model of the leading-edge flow showing the shear layer and the free-stream regions.

ordinates the shock is stationary, the flow becomes steady, and the wall slides past the foot of the shock wave with the propagation velocity $\bar{u}_1$.

In approaching the leading-edge problem it is important to recognize that the moving wall makes the shock-induced boundary layer fundamentally different from the classical boundary layer on a stationary flat plate. When the shock is weak, the wall velocity $\bar{u}_1$ is close to the free stream velocity $\bar{u}_2$, so that

$$(\bar{u}_1 - \bar{u}_2)/\bar{u}_1 \ll 1; \qquad (\bar{u}_1 - \bar{u}_2)/\bar{u}_2 \ll 1, \tag{1}$$

which suggests that the boundary-layer equations may be linearized. Mirels[6] has shown that the results of such linearization are in excellent agreement with exact solutions of the laminar boundary-layer equations when the shock is weak. On the other hand such linearization is never possible in the classical problem where the wall or plate is stationary.

There are also fundamental differences between the shock-induced and classical leading edges. In the classical problem the leading-edge singularity, which is introduced by the mathematically sharp edge of a semi-infinite plate, cannot be modified or softened by any physical arguments. No such "irrevocable" singularity is present in the shock-induced problem for the plate is infinite, the boundary layer being initiated by the velocity jump across the free-stream shock. This shock is not a mathematical discontinuity but has a finite thickness which varies inversely with the shock strength so that the sharpness of the shock-induced leading edge will depend upon the upstream Mach number, and the shock structure will dominate the leading-edge flow.

The difference between the two leading-edge problems can be formulated by comparing the boundary conditions. In the classical problem the boundary conditions at the plate are mixed and we have

$$\begin{aligned}
&\bar{u}(\bar{x}, 0) = 0, \quad \bar{v}(\bar{x}, 0) = 0, \quad \bar{x} > 0; \\
&\bar{u}_y(\bar{x}, 0) = 0, \quad \bar{v}(\bar{x}, 0) = 0, \quad \bar{x} < 0; \\
&\bar{u}(\bar{x}, \infty) = \bar{u}_e = \text{const}, \quad \bar{v}(\bar{x}, \infty) = 0, \\
&\qquad\qquad -\infty \leq x \leq \infty,
\end{aligned} \tag{2}$$

where $\bar{u}_e$ is the free-stream velocity, where dimensional quantities are barred, and where the subscript y denotes partial differentiation. On the other hand the boundary conditions for the shock-induced boundary layer are

$$\begin{aligned}
&\bar{u}(\bar{x}, 0) = \bar{u}_1, \quad \bar{v}(\bar{x}, 0) = 0, \\
&\qquad\qquad -\infty \leq \bar{x} \leq \infty; \\
&\bar{u}(\bar{x}, \infty) = \bar{u}_e(\bar{x}), \quad \bar{v}(\bar{x}, \infty) = 0, \\
&\qquad\qquad -\infty \leq \bar{x} \leq \infty,
\end{aligned} \tag{3}$$

and in the present case $\bar{u}_e$ is not constant but represents the velocity distribution within the free-stream shock.

The above comparison suggests that the shock-induced leading edge may be amenable to mathematical analysis if the free-stream shock is sufficiently weak. It may then be possible to linearize the leading-edge flow, and when the shock is weak, and hence relatively thick, some form of the boundary-layer approximation may remain valid even at the base of the shock wave. This possibility is supported by the work of Bertotti,[7] who showed that the boundary-layer equations remain valid at the foot of a shock wave standing outside the boundary layer on a semi-infinite flat plate provided the shock is sufficiently weak and close enough to the leading edge.

II. SHEAR LAYER

It is now postulated that the leading-edge flow may be subdivided into a shear layer near the wall

[6] H. Mirels, NACA TN 3401 (1955).

[7] B. Bertotti, Rend. ist. lombardo Sci. **A92**, 132 (1957).

where the transverse shear stress $\bar{\mu}(\partial\bar{u}/\partial\bar{y})$ is dominant, and a free-stream or shock region where the longitudinal viscous stress, $\bar{\mu}''(\partial\bar{u}/\partial\bar{x})$ is most important. A schematic diagram of this theoretical model is shown in Fig. 1(c). It is assumed that the fluid behaves as a continuum, and that relaxation effects are small enough to be accounted for by a bulk viscosity. Then the two-dimensional Navier–Stokes equations for a compressible fluid provide a mathematical description of the flow and are as follows:

$$\frac{D\bar{\rho}}{D\bar{t}} + \bar{\rho}\left(\frac{\partial\bar{u}}{\partial\bar{x}} + \frac{\partial\bar{v}}{\partial\bar{y}}\right) = 0, \tag{4}$$

$$\bar{\rho}\frac{D\bar{u}}{D\bar{t}} = -\frac{\partial\bar{p}}{\partial\bar{x}} + \frac{\partial}{\partial\bar{y}}\left(\bar{\mu}\frac{\partial\bar{u}}{\partial\bar{y}}\right) + \frac{\partial}{\partial\bar{x}}\left(\bar{\mu}''\frac{\partial\bar{u}}{\partial\bar{x}}\right) + \frac{\partial}{\partial\bar{y}}\left(\bar{\mu}\frac{\partial\bar{v}}{\partial\bar{x}}\right) + \frac{\partial}{\partial\bar{x}}\left[(\bar{\mu}'' - 2\bar{\mu})\frac{\partial\bar{v}}{\partial\bar{y}}\right], \tag{5}$$

$$\bar{\rho}\frac{D\bar{v}}{D\bar{t}} = -\frac{\partial\bar{p}}{\partial\bar{y}} + \frac{\partial}{\partial\bar{x}}\left(\bar{\mu}\frac{\partial\bar{v}}{\partial\bar{x}}\right) + \frac{\partial}{\partial\bar{y}}\left(\bar{\mu}''\frac{\partial\bar{v}}{\partial\bar{y}}\right) + \frac{\partial}{\partial\bar{x}}\left(\bar{\mu}\frac{\partial\bar{u}}{\partial\bar{y}}\right) + \frac{\partial}{\partial\bar{y}}\left[(\bar{\mu}'' - 2\bar{\mu})\frac{\partial\bar{u}}{\partial\bar{x}}\right], \tag{6}$$

$$\bar{\rho}\bar{T}\frac{D\bar{S}}{D\bar{t}} = \frac{\partial}{\partial\bar{x}}\left(\bar{k}\frac{\partial\bar{T}}{\partial\bar{x}}\right) + \frac{\partial}{\partial\bar{y}}\left(\bar{k}\frac{\partial\bar{T}}{\partial\bar{y}}\right) + \bar{\Phi}. \tag{7}$$

The viscous dissipation function $\bar{\Phi}$ is defined by

$$\bar{\Phi} = \bar{\mu}\left(\frac{\partial\bar{v}}{\partial\bar{x}} + \frac{\partial\bar{u}}{\partial\bar{y}}\right)^2 + 2\bar{\mu}\left(\frac{\partial\bar{u}}{\partial\bar{x}}\right)^2 + 2\bar{\mu}\left(\frac{\partial\bar{v}}{\partial\bar{y}}\right)^2 + (\bar{\mu}'' - 2\bar{\mu})\left(\frac{\partial\bar{u}}{\partial\bar{x}} + \frac{\partial\bar{v}}{\partial\bar{y}}\right)^2. \tag{8}$$

$\bar{\mu}''$ is the longitudinal viscosity which is related to the bulk viscosity $\bar{\mu}'$ and the shear viscosity $\bar{\mu}$ by[8]

$$\bar{\mu}'' = \tfrac{4}{3}\bar{\mu} + \bar{\mu}'. \tag{9}$$

In addition to the conservation equations the following thermodynamic relations are valid for any fluid[9]:

$$d\bar{p} = \bar{a}^2\, d\bar{\rho} + (\bar{\alpha}\bar{T}\bar{\rho}\bar{a}^2/\bar{c}_p)\, d\bar{S}, \tag{10}$$

$$\bar{c}_p\, d\bar{T} - \bar{T}\, d\bar{S} = (\bar{\alpha}\bar{T}/\bar{\rho})\, d\bar{p}, \tag{11}$$

$$\bar{\alpha}\bar{T} = (\gamma - 1)\bar{c}_p/\bar{a}^2\bar{\alpha}, \tag{12}$$

where $\bar{\alpha}$, the coefficient of thermal expansion, is defined by

$$\bar{\alpha} = \bar{\rho}\left[\frac{\partial(1/\bar{\rho})}{\partial\bar{T}}\right]_{\bar{p}}. \tag{13}$$

An expansion in the small parameter

$$\epsilon = M_1^* - 1, \tag{14}$$

which is proportional to the shock strength, coupled with stretching on the $\bar{x}$ and $\bar{y}$ coordinates will be used to attack the complicated system of equations above. Such a procedure is equivalent to an order-of-magnitude analysis.

The shock thickness $\bar{\lambda}$ and the shear-layer thickness $\bar{\delta}$, at the downstream edge of the shock wave, are the characteristic dimensions of the theoretical model depicted in Fig. 1(c). This suggests that the $\bar{x}$ and $\bar{y}$ coordinates be stretched or normalized according to

$$x = \bar{x}/\bar{\lambda}; \qquad y = \bar{y}/\bar{\delta}. \tag{15}$$

The shock thickness $\bar{\lambda}$ is taken as[10]

$$\bar{\lambda} = \nu_*''/a_*\epsilon, \tag{16}$$

where the asterisk refers to critical conditions where the fluid velocity equals the local speed of sound. The shear-layer thickness $\bar{\delta}$ is not known *a priori* but is determined later by the requirement that certain terms of the conservation equations be retained. An important feature of the normalization (15) is that the stretch factor $\bar{\lambda}$ is a function of the expansion parameter ϵ.

The flow variables are made dimensionless using critical conditions as a reference except for dimensionless pressure which is defined as

$$p = \bar{p}/\rho_* a_*^2. \tag{17}$$

The reference values, which are indicated by an asterisk, are those which would be reached if the flow upstream of the shock expanded isentropically to a Mach number equal to unity.

It is assumed that the wall temperature is constant and equal to T_1 the temperature upstream of the shock wave, an assumption which is justified by the calculations of Rott and Hartunian.[11] The wall moves with the upstream velocity, which in dimensionless form is given by $u_1 = 1 + \epsilon$, and

[8] W. D. Hayes, *Fundamentals of Gas Dynamics* (Princeton University Press, Princeton, New Jersey, 1958), Sec. D.

[9] F. W. Sears, *Thermodynamics* (Addison-Wesley Publishing Company, Inc., Reading, Massachusetts, 1953), pp. 147–151.

[10] M. J. Lighthill, "Viscosity in Waves of Finite Amplitude," in *Surveys in Mechanics*, edited by G. K. Batchelor and R. M. Davis (Cambridge University Press, New York, 1956).

[11] N. Rott and R. A. Hartunian, *On the Heat Transfer to the Walls of a Shock Tube* (Cornell University Press, Ithaca, New York, 1955).

the free-stream velocity downstream of the shock is $u_2 = 1 - \epsilon$ to first order in ϵ. Since entropy changes in the weak free-stream shock wave are of higher order, the free-stream pressure, density, temperature, and velocity are according to Hayes,[8] related by

$$\begin{aligned} d\bar{p} &\cong -\bar{p}\bar{u}\, d\bar{u}, \\ \bar{c}_p\, d\bar{T} &\cong (\bar{\alpha}\bar{T}/\bar{p})\, d\bar{p}, \\ d\bar{p} &\cong \bar{a}^2\, d\bar{\rho}. \end{aligned} \tag{18}$$

These considerations suggest expansion of the quantities u, p, T, μ, μ'', c_p, α, and k in series of the form

$$L = 1 + \epsilon L^{(1)} + \epsilon^2 L^{(2)} + \cdots + \epsilon^n L^{(n)} + \cdots, \tag{19}$$

where L symbolizes the parameter in question. Because $\rho_*(a_*)^2$ rather than p_* is used as a reference, the expansion for p takes the form

$$p = (1/\gamma_*) + \epsilon p^{(1)} + \epsilon^2 p^{(2)} + \cdots + \epsilon^n p^{(n)} + \cdots. \tag{20}$$

Consideration of the y component of velocity, v, is left until later.

Substituting the stretched coordinates and the series (19) and (20) into the conservation equations and keeping only the largest terms, the continuity and momentum equations become

$$\epsilon^2 \frac{\partial \rho^{(1)}}{\partial x} + \frac{\epsilon}{\mathcal{R}'} v \frac{\partial \rho^{(1)}}{\partial y} + \epsilon^2 \frac{\partial u^{(1)}}{\partial x} + \frac{1}{\mathcal{R}'} \frac{\partial v}{\partial y} = 0, \tag{21}$$

$$\epsilon^2 \frac{\partial u^{(1)}}{\partial x} + \frac{\epsilon}{\mathcal{R}'} v \frac{\partial u^{(1)}}{\partial y} = -\epsilon^2 \frac{\partial p^{(1)}}{\partial x} + \frac{\epsilon}{\mathcal{R}\mathcal{R}'} \frac{\partial^2 u^{(1)}}{\partial y^2} + \epsilon^3 \frac{\partial^2 u^{(1)}}{\partial x^2} + \epsilon\left(\frac{1}{\mathcal{R}'} - \frac{1}{\mathcal{R}}\right) \frac{\partial^2 v}{\partial y\, \partial x}, \tag{22}$$

where

$$\mathcal{R} = a_* \bar{\delta}/\nu_*, \qquad \mathcal{R}'' = a_* \bar{\delta}/\nu''_*.$$

The terms $(1/\mathcal{R}'')(\partial v/\partial y)$ and $(\epsilon/\mathcal{R}\mathcal{R}'')(\partial^2 u^{(1)}/\partial y^2)$ must be retained in Eqs. (21) and (22) and should be of the same order as $\epsilon^2(\partial u^{(1)}/\partial x)$ and $\epsilon^2(\partial \rho^{(1)}/\partial x)$. Otherwise these equations will yield the inconsistent result that pressure and density variations at the base of the shock are $O(\epsilon^2)$, whereas it is known from Mirels' boundary-layer solution[6] and the Hugoniot conditions that the over-all pressure and density change is $O(\epsilon)$. If the terms $(\epsilon v/\mathcal{R}'')(\partial \rho^{(1)}/\partial y)$ and $(\epsilon v/\mathcal{R}'')(\partial u^{(1)}/\partial y)$ were the ones retained, then $(1/\mathcal{R}'')(\partial v/\partial y)$ and $(\epsilon/\mathcal{R}\mathcal{R}'')(\partial^2 u^{(1)}/\partial y^2)$ would be larger than any of the other terms in Eqs. (21) and (22).

To retain $(1/\mathcal{R}'')(\partial v/\partial y)$ and $(\epsilon/\mathcal{R}\mathcal{R}'')(\partial^2 u^{(1)}/\partial y^2)$ in the continuity and momentum equations it is necessary that

$$v/\mathcal{R}'' \sim O(\epsilon^2), \qquad 1/\mathcal{R}\mathcal{R}'' \sim O(\epsilon), \tag{23}$$

or, using the definitions of $\mathcal{R}$ and $\mathcal{R}''$, that

$$\begin{aligned} \bar{\delta} &\sim O[(1/a_*)(\nu_*\nu''_*/\epsilon)^{\frac{1}{2}}], \\ v &\sim O[\epsilon^{\frac{1}{2}}(\nu_*/\nu''_*)^{\frac{1}{2}}]. \end{aligned} \tag{24}$$

Equations (24) and (16) show that when the order-of-magnitude analysis is valid

$$\bar{\delta}/\bar{\lambda} \sim O[\epsilon^{\frac{1}{2}}(\nu_*/\nu''_*)^{\frac{1}{2}}], \tag{25}$$

that is, the shear layer will be much thinner than the shock wave when the shock is sufficiently weak. On the basis of Eq. (24), the vertical velocity v is now expanded in the series

$$v = \epsilon^{\frac{1}{2}}(\epsilon v^{(1)} + \epsilon^2 v^{(2)} + \cdots). \tag{26}$$

By using the order-of-magnitude results above, and eliminating the entropy from the energy equation (7) with the thermodynamic relation (11), the following set of equations is obtained for the first-order coefficients of the expansion in ϵ:

$$\text{continuity:} \quad \frac{\partial \rho^{(1)}}{\partial x} + \frac{\partial u^{(1)}}{\partial x} + \frac{1}{\beta} \frac{\partial v^{(1)}}{\partial y} = 0, \tag{27}$$

$$x \text{ momentum:} \quad \frac{\partial u^{(1)}}{\partial x} = -\frac{\partial p^{(1)}}{\partial x} + \frac{\partial^2 u^{(1)}}{\partial y^2}, \tag{28}$$

$$y \text{ momentum:} \quad \frac{\partial p^{(1)}}{\partial y} \sim O(\epsilon), \tag{29}$$

$$\text{energy:} \quad \frac{\partial T^{(1)}}{\partial x} = \frac{(\gamma_* - 1)}{\alpha_* T_*} \frac{\partial p^{(1)}}{\partial x} + \frac{1}{\mathrm{Pr}_*} \frac{\partial^2 T^{(1)}}{\partial y^2}. \tag{30}$$

In the above equations $\beta = (\nu_*/\nu''_*)$ and Pr_* is the Prandtl number at the critical or reference condition. Finally the thermodynamic relations (10), (11), and (12) yield the following relation between $p^{(1)}$, $\rho^{(1)}$, and $T^{(1)}$:

$$\gamma_*\, dp^{(1)} = d\rho^{(1)} + \alpha_* T_*\, dT^{(1)}. \tag{31}$$

It should be observed that for a perfect gas $\alpha_* T_* = 1$. In the work below the asterisk of γ_* will be suppressed, and γ represents the ratio of specific heats at the reference conditions.

From the free-stream thermodynamic relations (18) and the conditions at the wall, it follows that

the first-order shear-layer equations (27)–(31) must have the boundary conditions

$$\begin{aligned} u^{(1)}(x, 0) &= u^{(1)}(-\infty, y) = +1, \\ u^{(1)}(x, \infty) &= u_e^{(1)}(x), \qquad v^{(1)}(x, 0) = 0, \\ T^{(1)}(x, 0) &= T^{(1)}(-\infty, y) = -(\gamma - 1)/\alpha_* T_*, \\ T^{(1)}(x, \infty) &= T_e^{(1)}(x) = -[(\gamma - 1)/\alpha_* T_*] u_e^{(1)}(x), \end{aligned} \tag{32}$$

where $u_e^{(1)}$ represents the variation of $u^{(1)}$ at the outer edge of the shear layer.

Equations (27)–(30) with the associated boundary conditions (32) may be recognized as the linearized boundary-layer equations used by Mirels[6] with, however, a variable free-stream pressure. A key result of the analysis is thus that the boundary-layer approximation with its accompanying simplifications may be extended even to the base of the shock wave provided the shock is sufficiently weak. The reason that this extension is possible is that as the upstream Mach number approaches unity the shock becomes much thicker than the shear layer. The shear-layer equations are linear because in the case of a weak shock the plate moves with a velocity which is not very different from that of the free stream.

The order of the magnitude of the shear-layer thickness may also be established by analogy with the results of Rayleigh[12] for a sound wave moving down a two-dimensional channel. It seems reasonable to suppose that the shear layer at the foot of a weak shock wave moving past a wall does not differ drastically from the viscous layer which sinusoidal acoustic waves generate on the wall of a two-dimensional channel. Rayleigh found that the thickness $\bar{d}$ of this layer is

$$\bar{d} \sim O(\bar{\nu}\bar{l}/\bar{a})^{\frac{1}{2}}, \tag{33}$$

where $\bar{l}$ is the wavelength. If now $\bar{l}$ is replaced by the shock thickness $\bar{\lambda}$ it follows from Eq. (16) for the order of magnitude of $\bar{\lambda}$ that

$$\bar{d} \sim O(\bar{\nu}\bar{\lambda}/\bar{a})^{\frac{1}{2}} = (1/a_*)(\nu_* \nu'_*/\epsilon)^{\frac{1}{2}}, \tag{34}$$

which is the same as the result obtained in Eq. (24) above.

III. SOLUTION OF THE SHEAR-LAYER EQUATIONS

Since entropy changes are of higher order in the free stream and since $\partial p^{(1)}/\partial y \sim O(\epsilon)$ it follows from the first of equations (18) that the momentum equation can be written

$$\partial u^{(1)}/\partial x = du_e^{(1)}/dx + \partial^2 u^{(1)}/\partial y^2. \tag{28a}$$

Equation (28a) is the well-known diffusion or heat-conduction equation, which is extensively treated by Carslaw and Jaeger.[13] The boundary conditions (32) differ from those of conventional heat-transfer problems in which x is interpreted as time and restricted to $x \geq 0$. In the present case with x interpreted as a coordinate there is no reason why the above restriction should be necessary. Equation (28a) subject to the boundary conditions (32) has the solution

$$u^{(1)} = u_e^{(1)}(x) + 1 - \frac{2}{\pi^{\frac{1}{2}}} \int_0^\infty u_e^{(1)}\left(x - \frac{y^2}{4w^2}\right) \exp(-w^2)\, dw. \tag{35}$$

A comparison of the energy equation (30) with the momentum equation (28a) combined with the boundary conditions (32) leads to the following energy integral relating $u^{(1)}$ and $T^{(1)}$:

$$T^{(1)}(x, y) = -[(\gamma - 1)/\alpha_* T_*] u^{(1)}(x, y\mathrm{Pr}^{\frac{1}{2}}). \tag{36}$$

Equation (36) is in accord with the result[14] that the ratio of the thickness of the velocity boundary layer to the thickness of the thermal boundary layer is of the order of $\mathrm{Pr}^{\frac{1}{2}}$.

The vertical velocity $v^{(1)}(x, y)$ may now be determined from the continuity equation (27) by using Eq. (31) to eliminate the density $\rho^{(1)}$ with the result that

$$v^{(1)}(x, y) = \frac{2\beta}{\pi^{\frac{1}{2}}} \int_0^y \int_0^\infty \left[(\gamma - 1) u'_e\left(x - \frac{\mathrm{Pr}\, y^2}{4w^2}\right) + u'_e\left(x - \frac{y^2}{4w^2}\right)\right] \exp(-w^2)\, dw\, dy, \tag{37}$$

where the prime here denotes differentiation. This result will be valid as long as $u_e(x)$ and $u'_e(x)$ remain bounded. In the above, the superscript of $u_e^{(1)}$ has been suppressed. From Eq. (37) it may be shown[15] that

[12] Lord Rayleigh, *Theory of Sound* (Dover Publications, New York, 1896), Vol. II, p. 334.

[13] H. S. Carslaw and J. C. Jaeger, *Conduction of Heat in Solids* (Oxford University Press, New York, 1958), 2nd ed.

[14] L. Howarth, *Modern Developments in Fluid Dynamics, High Speed Flow* (Oxford University Press, New York, 1953), Vol. I.

[15] M. Sichel, "A Study of the Leading Edge of a Shock Induced Boundary Layer," Ph.D. thesis, Princeton University (1961).

$$\lim_{y\to\infty} v^{(1)}(x, y) = v^{(1)}(x, \infty)$$
$$= \beta\pi^{-\frac{1}{2}}[1 + (\gamma - 1)\,\mathrm{Pr}^{-\frac{1}{2}}] \cdot \int_{-\infty}^{x} u_e'(\xi)(x - \xi)^{-\frac{1}{2}}\, d\xi. \tag{38}$$

The above is a key result for the flow in the free stream or shock region adjacent to the shear layer depends upon $v^{(1)}(x, \infty)$, the velocity at the outer edge of the shear layer.

With $u^{(1)}$, $T^{(1)}$, and $v^{(1)}$ known, other shear-layer parameters are readily determined. Thus the wall shear stress $\bar{\tau}(x, 0)$ and heat-transfer rate $\bar{q}(x, 0)$ are related to the vertical velocity $v^{(1)}(x, \infty)$ by

$$\bar{\tau}(x, 0) = \frac{\mathrm{Pr}^{\frac{1}{2}}}{a_*\alpha_* T_*}\,\bar{q}(x, 0) = \frac{\rho_* a_*^2 \epsilon^{\frac{1}{2}} v^{(1)}(x, \infty)}{[1 + (\gamma - 1)\,\mathrm{Pr}^{-\frac{1}{2}}]}, \tag{39}$$

where

$$\bar{\tau}(x, y) = \bar{\mu}(\partial\bar{u}/\partial\bar{y}), \qquad \bar{q}(x, y) = -\bar{k}(\partial\bar{T}/\partial\bar{y}).$$

The relation (39) is essentially a Reynolds analogy between heat transfer and shear stress at the wall.

A displacement thickness $\bar{\delta}_1$ and a momentum thickness $\bar{\theta}_1$ may also be defined for the shear layer. To make $\bar{\delta}_1$ and $\bar{\theta}_1$ positive the definition introduced by Rott and Hartunian[11] is used so that to first order

$$\bar{\delta}_1 = \int_0^\infty \left(\frac{\bar{\rho}\bar{u}}{\bar{\rho}_e\bar{u}_e} - 1\right) d\bar{y} = \frac{(\epsilon\nu_*\nu_*'')^{\frac{1}{2}}}{a_*}\int_0^\infty (\rho^{(1)} + u^{(1)})\, dy.$$
$$\bar{\theta}_1 = \int_0^\infty \frac{\bar{\rho}\bar{u}}{\bar{\rho}_e\bar{u}_e}\left(\frac{\bar{u}}{\bar{u}_e} - 1\right) d\bar{y} = \frac{(\epsilon\nu_*\nu_*'')^{\frac{1}{2}}}{a^*}\int_0^\infty (u^{(1)} - u_e^{(1)})\, dy. \tag{40}$$

Comparison of Eqs. (40) and (24) shows the interesting result that the displacement and momentum thicknesses are an order of magnitude smaller than the shear-layer thickness since $\bar{\delta}_1/\bar{\delta}$ and $\bar{\theta}_1/\bar{\delta}$ are $O(\epsilon)$. By contrast for the conventional boundary layer (such as on a stationary flat plate) the displacement, momentum, and boundary-layer thicknesses are of the same order of magnitude. The above anomaly is caused by the moving-wall boundary condition and the fact that whereas $\bar{\delta}_1$ represents a mass flow change due to the viscous layer, $\bar{\delta}$ represents the distance in which the velocity changes from $\bar{u}_1$ at the wall to $\bar{u}_e$. Thus as ϵ decreases, $\bar{\delta}$ increases even though the additional mass flow carried by the viscous layer decreases.

From the solution for $u^{(1)}$, $\rho^{(1)}$, and $v^{(1)}$, it now follows that

$$d\delta_1/dx = -(1/\beta)v^{(1)}(x, \infty), \qquad \delta_1/\theta_1 = 1 + (\gamma - 1)\,\mathrm{Pr}^{-\frac{1}{2}}, \tag{41}$$

where

$$\delta_1 = a_*\,\bar{\delta}_1(\epsilon\nu_*\nu_*'')^{-\frac{1}{2}}, \qquad \theta_1 = a_*\bar{\theta}_1(\epsilon\nu_*\nu_*'')^{-\frac{1}{2}}.$$

Equation (41) shows that the shear layer behaves like a very slender body with respect to the free stream and that the ratio of displacement to momentum thickness is constant. The basic parameters of the shear layer are now established, and it becomes necessary to determine whether the solution obtained above is physically reasonable.

The shear-layer theory was developed to bridge the gap between the undisturbed region upstream of the shock and the fully developed downstream boundary-layer flow. Since the shear-layer equations are the same as Mirels' linearized boundary-layer equations with a variable free-stream pressure it seems reasonable that the solution of the shear-layer equations will approach Mirels' solution

$$u^{(1)} = -1 + 2\,\mathrm{erf}\,(y/2x^{\frac{1}{2}}),$$
$$v^{(1)} = -\frac{2\beta}{(\pi x)^{\frac{1}{2}}}\left\{\left[1 - \exp\left(-\frac{y^2}{4x}\right)\right] + \frac{\gamma - 1}{\mathrm{Pr}^{\frac{1}{2}}}\left[1 - \exp\left(-\frac{y^2\,\mathrm{Pr}}{4x}\right)\right]\right\}, \tag{42}$$
$$\delta_1 = 4(x/\pi)^{\frac{1}{2}}[1 + (\gamma - 1)\,\mathrm{Pr}^{-\frac{1}{2}}],$$

provided that $u_e^{(1)}(x)$ approaches the downstream Hugoniot condition, $u_e(\infty) = -1$, fast enough. It can be shown rigorously that Eqs. (42) describe the asymptotic behavior of the solution for $u^{(1)}$ and $v^{(1)}$ in Eqs. (35) and (37) as $x \to \infty$.[15]

The behavior of the solution as $x \to -\infty$ also is of interest, and again depends upon $u_e^{(1)}(x)$. As shown later, as $x \to -\infty$, $u_e^{(1)}(x)$ may resemble Taylor's solution for the structure of weak shocks so that[8]

$$u_e^{(1)}(x) = -\tanh cx \approx 1 + 2\sum_{n=1}^{\infty}(-1)^n e^{2ncx} \quad \text{as} \quad x \to -\infty, \tag{43}$$

where C is a constant depending upon Pr, γ, and in the case of oblique shocks upon the shock angle.

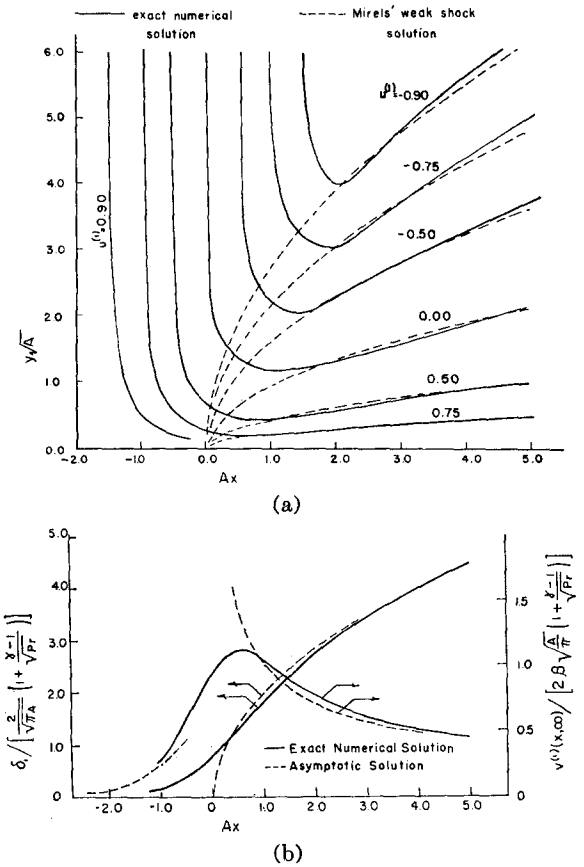

FIG. 2. (a) Isotachs ($u^{(1)}$ = const) within the shear layer with $u_e^{(1)} = -\tanh Ax$; (b) Shear-layer displacement thickness δ_1 and vertical velocity $v^{(1)}(x, \infty)$ at the outer edge of the shear layer, with $u_e^{(1)} = -\tanh Ax$.

From Eqs. (43), (35), (37), and (41) it follows that

$$u^{(1)}(x, y) \underset{x\to-\infty}{\sim} 1 + 2\sum_{n=1}^{\infty}(-1)^n e^{2ncx} \{1 - \exp[-y(2nc)^{\frac{1}{2}}]\},$$

$$v^{(1)}(x, \infty) \underset{x\to-\infty}{\sim} 2\beta c^{\frac{1}{2}}[1 + (\gamma - 1)\,\mathrm{Pr}^{-\frac{1}{2}}] \cdot \sum_{n=1}^{\infty}(-1)^n (2n)^{\frac{1}{2}} e^{2ncx}, \qquad (44)$$

$$\delta_1 \underset{x\to-\infty}{\sim} 2[1 + (\gamma - 1)\,\mathrm{Pr}^{-\frac{1}{2}}] \cdot \sum_{n=1}^{\infty}(-1)^{n+1}(2nc)^{-\frac{1}{2}} e^{2ncx}.$$

It is interesting to compare Mirels' solution (42) and the asymptotic solution (44). As $x \to \infty$ all quantities become functions of the boundary-layer similarity variable $y/x^{\frac{1}{2}}$; however, no such variable is evident in the solution for $x \to -\infty$.

Even though the exact variation of $u_e^{(1)}(x)$, which depends on the interaction between the free stream and the shear layer, is unknown, calculations of $v^{(1)}$ and $u^{(1)}$ with $u_e^{(1)}(x)$ corresponding to a weak normal shock were made since these give an indication of the order of magnitude and over-all behavior of $u^{(1)}$ and $v^{(1)}$. In the case of a weak normal shock $u_e^{(1)}$ corresponds to Taylor's solution mentioned above so that[8]

$$u_e^{(1)}(x) = -\tanh Ax,$$

$$A = \tfrac{1}{2}(\gamma - 1)[1 + (\gamma - 1)/\mathrm{Pr}'']^{-1}, \qquad (45)$$

and the actual behavior of $u_e^{(1)}(x)$ should not differ drastically from this. Using $u_e^{(1)}(x)$ in (45), $u^{(1)}(x, y)$ and $v^{(1)}(x, \infty)$ were determined numerically from Eqs. (35) and (38) and the results are shown in Figs. 2(a) and 2(b).

The isotach diagram in Fig. 2(a) shows the transition from the free-stream flow to the shear-layer structure. As in the conventional boundary layer with pressure gradient, the shear-layer approximation is valid, i.e.,

$$\frac{\partial u^{(1)}/\partial x}{\partial u^{(1)}/\partial y} \leq O(1),$$

except at the outer edge where the shear-layer and free-stream flows merge.

Figure 2(b) shows both the asymptotic and shear-layer values of $v^{(1)}(x, \infty)$ and δ_1. $v^{(1)}(x, \infty)$ has a maximum because the streamlines curve sharply toward the wall when they first enter the shear layer. δ_1 increases smoothly from zero rather than being represented by a parabola with infinite slope at the leading edge, as in the conventional boundary-layer theory.

The properties of nitrogen were used for a sample[10] calculation to indicate the order of magnitude of $v^{(1)}(x, \infty)$. For N_2 at 25°C $\mu' = 0.8\,\mu$, Pr = 0.75, and $\gamma = 1.40$. From these values it follows that $A = 0.960$, $\mathrm{Pr}'' = 1.60$, $\beta = 0.685$, and $v^{(1)}(x, \infty)$ has a maximum value of 1.12.

Both Fig. 2(a) and 2(b) show that the shear-layer theory provides a physically reasonable connecting link between the undisturbed upstream region and the downstream boundary layer.

IV. FREE STREAM

The velocity $v(x, \infty)$ at the outer edge of the shear layer is of the same order as the vertical velocity in a transonic oblique shock [i.e., of $O(\epsilon^{\frac{1}{3}})$]; therefore, a normal shock structure with $v(x, y) = 0$ cannot represent the free-stream or shock-region flow. Rather, the free-stream shock structure and the shear layer must interact. The possibility that at the edge of the shear layer the free stream could

be exactly represented by an oblique shock is ruled out for there is no reason why the oblique shock variation of $v^{(1)}$ and the velocity $v^{(1)}(x, \infty)$ generated by the shear layer should match. The shock structure must therefore be two dimensional near the outer edge of the shear layer.

Sternberg[16] has mentioned such a region with a two-dimensional shock structure in his study of the Mach reflection of weak shock waves. At the triple intersection between the incident and reflected waves and the Mach stem, there is a transition between the structure of the incident and reflected waves above the triple point and the structure of the Mach stem which lies below the triple point, and thus the structure must be two dimensional. Sternberg referred to this region as a non-Rankine–Hugoniot shock wave. Since a weak non-Hugoniot shock region is involved in both the Mach reflection and the present problem, one may expect that the two non-Hugoniot flows will have many similarities.

From an order-of-magnitude analysis of the Navier–Stokes equations it may be shown[15] that the first-order flow in the non-Hugoniot shock region may, for a perfect gas, be described by the equations

$$\left(1 + \frac{\gamma - 1}{\mathrm{Pr}''}\right)\frac{\partial^2 u^{(1)}}{\partial x^2} - (\gamma + 1)u^{(1)}\frac{\partial u^{(1)}}{\partial x} + \frac{\partial v^{(1)}}{\partial \hat{y}} = 0,$$

$$\partial v^{(1)}/\partial x = \partial u^{(1)}/\partial \hat{y}, \tag{46}$$

where $\hat{y}$, the stretched free-stream coordinate, is related to y by

$$\hat{y} = \bar{y} a_* \epsilon^{\frac{1}{2}}/\nu''_*.$$

It has not been possible to find a solution of the above nonlinear set of free-stream equations subject to the boundary conditions imposed by the interaction with the shear layer. Consequently the detailed derivation of (46) will not be presented here.

To obtain a solution of the leading-edge problem, the free-stream flow will therefore be approximated by an oblique shock which is matched to the shear-layer flow at only one point. The shear layer has the effect of removing fluid from the free stream; hence, $v^{(1)} < 0$ and the oblique shock must be inclined in an upstream direction as shown in Fig. 1(a). Since the shock is transonic, σ, the angle between the shock and the vertical, is $O(\epsilon^{\frac{1}{2}})$. The Hugoniot conditions across a transonic oblique shock are well known[17] and in the present notation are

$$\begin{aligned} u_1^{(1)} &= +1, \qquad u_2^{(1)} = -1 + 2\alpha^2(\gamma + 1)^{-1}, \\ v_1^{(1)} &= 0, \qquad v_2^{(1)} = -2\alpha[1 - \alpha^2(\gamma + 1)^{-1}], \end{aligned} \tag{47}$$

where α, the obliquity parameter, is $O(1)$, and is defined by

$$\sigma = \alpha\epsilon^{\frac{1}{2}},$$

and where subscripts 1 and 2 refer to upstream and downstream conditions.

An oblique shock may be derived from a normal shock wave by superimposing a velocity which is parallel to the wave on the over-all flow. Hence, it is readily shown that the structure of a weak or transonic oblique shock wave may be described by the equations

$$\begin{aligned} u^{(1)}(x, \hat{y}) &= \frac{\alpha^2}{\gamma + 1} - \left(1 - \frac{\alpha^2}{\gamma + 1}\right) \\ &\quad \cdot \tanh A\left(1 - \frac{\alpha^2}{\gamma + 1}\right)(x + \alpha\hat{y}), \\ v^{(1)}(x, \hat{y}) &= -\alpha\left(1 - \frac{\alpha^2}{\gamma + 1}\right) \\ &\quad \cdot \left[1 + \tanh A\left(1 - \frac{\alpha^2}{\gamma + 1}\right)(x + \alpha\hat{y})\right]. \end{aligned} \tag{48}$$

When $\alpha \to 0$ the oblique shock structure above reduces to the Taylor structure of a weak normal shock wave. Equation (48) satisfies the Hugoniot conditions as $x \to \pm\infty$. As σ approaches the Mach angle, which is given by

$$\begin{aligned} \sigma_M &= \tan^{-1}(M_1^2 - 1)^{\frac{1}{2}} \approx \epsilon^{\frac{1}{2}}(\gamma + 1)^{\frac{1}{2}}, \\ \alpha_M &= (\gamma + 1)^{\frac{1}{2}}, \end{aligned} \tag{49}$$

it can be seen from (48) that the oblique shock degenerates to an infinitesimal acoustic wave as is to be expected. The value of α for which $v_2^{(1)}$ is a maximum may be determined from Eq. (47) and is

$$\alpha_{\max} = [\tfrac{1}{3}(\gamma + 1)]^{\frac{1}{2}},$$

while

$$v_{2\max}^{(1)} = -\tfrac{4}{3}[\tfrac{1}{3}(\gamma + 1)]^{\frac{1}{2}}.$$

In a transonic oblique shock $\alpha_{\max}$ and the value of α at shock detachment coincide.[18] It should also be mentioned that $u^{(1)}$ and $v^{(1)}$ in (48) satisfy the free-stream equations (46), as is to be expected since the conditions in a transonic oblique shock are similar to those used in the order-of-magnitude analysis which led to the derivation of (46).

[16] J. Sternberg, Phys. Fluids **2**, 179 (1959).

[17] K. Oswatitsch, *Gas Dynamics* (Academic Press Inc., New York, 1956).

[18] K. G. Guderley, *Theorie schallnaher Strömungen* (Springer-Verlag, Berlin, 1957).

In the present case the oblique shock used to approximate the free-stream flow is curved so that the obliquity parameter α is a function of $\hat{y}$, i.e., $\alpha = \alpha(\hat{y})$. The variation of α with $\hat{y}$ is related to the shock radius of curvature since

$$\frac{1}{\bar{R}} = \frac{d\sigma}{d\bar{y}} = \epsilon^2 \frac{a_*}{\nu_*''} \frac{d\alpha}{d\hat{y}}. \tag{50}$$

For the oblique shock structure (48) to remain valid the shock-wave curvature must not be too great. An upper limit to this curvature may be determined by considering the irrotationality condition

$$\partial u^{(1)}/\partial \hat{y} = \partial v^{(1)}/\partial x$$

which of course must be satisfied by $u^{(1)}$ and $v^{(1)}$ in (48). From (48) it can be seen that

$$v^{(1)}(x, \hat{y}) = \alpha[u^{(1)}(\xi) - 1], \tag{51}$$

where

$$\xi = x + \alpha\hat{y}.$$

Now taking variation of α into account we have the result

$$\frac{\partial u^{(1)}}{\partial \hat{y}} = \frac{du^{(1)}}{d\xi}\left(\alpha + \hat{y}\frac{d\alpha}{d\hat{y}}\right), \tag{52}$$

$$\partial v^{(1)}/\partial x = \alpha\, du^{(1)}/d\xi.$$

From Eq. (52) it can be seen that the oblique shock solution will satisfy the irrotationality condition only if $(d\alpha/d\hat{y})$ drops out of (52), i.e.,

$$d\alpha/d\hat{y} \sim O(\epsilon).$$

From this requirement it would appear the structure of a curved oblique shock will remain quasi-one dimensional only as long as $(1/\bar{R}) \sim O(\epsilon^3 a_*/\nu_*'')$, or, since the shock thickness $\bar{\lambda}$ is $O(\nu_*''/a_*\epsilon)$, as long as

$$\bar{\lambda}/\bar{R} \leq O(\epsilon^2). \tag{53}$$

The approximate solution developed below will thus be valid only in those regions in which the free-stream oblique shock satisfies the condition (53) developed above.

It is surprising that the ratio of shock thickness to shock radius $\bar{\lambda}/\bar{R}$ must be equal to or less than second order in ϵ for on first thought it would seem that $\bar{\lambda}/\bar{R} \leq O(\epsilon)$ should be sufficient. One explanation for this strange result lies in the fact that shock structure arises from a balance between the viscous and convective terms which in a weak shock are of second order[15] in ϵ. For the oblique shock solution to remain valid the shock curvature must be sufficiently small to make second-order variations parallel to the shock negligible and this requirement gives rise to condition (53).

V. APPROXIMATE SOLUTION OF THE LEADING-EDGE INTERACTION PROBLEM

To obtain an approximate solution of the leading-edge interaction it is necessary to match the shear-layer flow and the free-stream oblique shock. The shape of the free-stream shock wave is then determined from the inviscid solution for the flow between the downstream edge of the shock and the shear layer.

The matching of the free-stream shock wave and the shear layer will be considered first. Using $u^{(1)}(x, 0)$ from Eq. (48) as $u_e^{(1)}$ in Eq. (38) and introducing the transformation $\eta = [AB(x - \xi)]^{\frac{1}{2}}$ the following expression is obtained for $v^{(1)}(x, \infty)$:

$$v^{(1)}(x, \infty) = -2\beta(A/\pi)^{\frac{1}{2}}[1 + (\gamma - 1)\,\mathrm{Pr}^{-\frac{1}{2}}]B^{\frac{1}{2}} \cdot \int_0^\infty \mathrm{sech}^2\,(ABx - \eta^2)\, d\eta, \tag{54}$$

where

$$B = 1 - \alpha^2/(\gamma + 1).$$

The integral in (54) also occurs in the shear-layer solution for a Taylor shock in the free stream, and if Ax in Fig. 2(b) is replaced by ABx, the curve of

$$v^{(1)}(x, \infty)/2\beta(A/\pi)^{\frac{1}{2}}[1 + (\gamma - 1)\,\mathrm{Pr}^{-\frac{1}{2}}]$$

represents a plot of the integral in (54).

In this approximate-solution scheme the method of matching is somewhat arbitrary. In the present case, the matching obliquity parameter α_m was chosen so that the vertical velocity $v_2^{(1)}$ downstream of the shock equals the maximum value of $v^{(1)}(x, \infty)$ [see Fig. 2(b)]. Since the integral in (54) has a maximum of 1.12, comparison of (54) and (47) shows that

$$\alpha_m = (\gamma + 1)^{\frac{1}{2}}[1 + 4(\gamma + 1)/(1.12\kappa)^2]^{-\frac{1}{2}}, \tag{55}$$

where

$$\kappa = 2\beta(A/\pi)^{\frac{1}{2}}[1 + (\gamma - 1)\,\mathrm{Pr}^{-\frac{1}{2}}].$$

α_m lies on the strong branch of the shock polar. The resultant shear layer and oblique shock velocity distributions computed using the properties of N_2 are shown in Fig. 3(a). For $Ax < 2$, i.e., at the base of the shock, the two velocity distributions are in reasonably good agreement, which provides some

justification for the matching criterion used. The results of matching the upstream asymptotic shear layer and oblique shock behavior is shown in Fig. 3(b) for comparison. Clearly this latter matching procedure is unacceptable.

The inviscid flow between the shock and the shear layer must now be determined. Entropy changes across the weak free-stream shocks are of higher order; therefore, the flow in this inviscid region, which is shown schematically in Fig. 4, is irrotational. Downstream of the shock wave it is convenient to write

$$u^{(1)} = -1 + u', \tag{56}$$

where u' is a perturbation of $u^{(1)}$ downstream of the free-stream normal shock. Because of irrotationality, a potential φ such that

$$u' = \varphi_x, \qquad v^{(1)} = \varphi_{\hat{y}}, \tag{57}$$

may be introduced, and in the present case this potential satisfies the transonic equation[18]

$$(\gamma + 1)\varphi_{xx} + \varphi_{\hat{y}\hat{y}} = (\gamma + 1)\varphi_x\varphi_{xx}. \tag{58}$$

The solution of the nonlinear transonic equation is a formidable job; however, in the present case the nonlinear term in (58) may be neglected because $v^{(1)}$, the disturbance at the base of the shock wave, is very small. It has already been remarked (Sec. III) that the shear layer acts like a thin body, and this body will have a thickness ratio τ of the order $\epsilon^{\frac{3}{4}}v_{\max}^{(1)}$, where $v_{\max}^{(1)}$ is the maximum vertical velocity

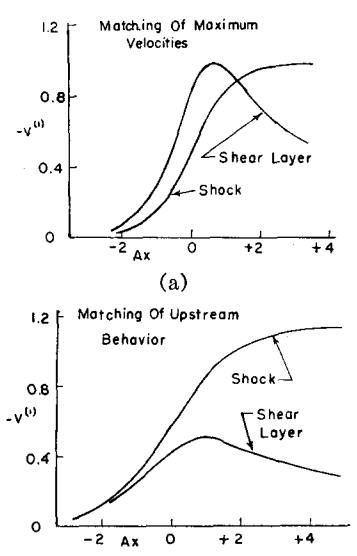

FIG. 3. Velocity profiles obtained in matching an oblique shock to the shear layer, and using the properties of N_2.

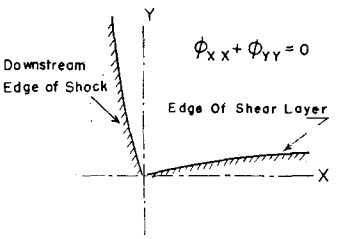

FIG. 4. Boundaries of the inviscid flow in the approximate solution of the leading-edge interaction problem.

in the shear layer. Cole[19] has shown that the ratio Q between the linear and nonlinear terms of the transonic equation as applied to the two-dimensional flow over a thin body with thickness ratio τ is approximately

$$Q = (\gamma + 1)M_2^2\tau/(1 - M_2^2)^{\frac{3}{2}},$$

where M_2 is the free-stream Mach number. In the present case the largest value of this ratio is

$$Q_{\max} = v_{\max}^{(1)}(\gamma + 1)^{-\frac{1}{2}}.$$

For most gases of interest $|Q_{\max}| < 1$, and both Cole[19] and Guderley[18] suggest that the nonlinear term of the transonic equation may reasonably be neglected if $|Q| < 1$. In the case of N_2 for example $|Q_{\max}| = 0.645$.

Without the nonlinear term, and with the transformation

$$Y = (\gamma + 1)^{\frac{1}{2}}\hat{y}, \qquad X = x,$$

Eq. (58) now reduces to the LaPlace equation

$$\varphi_{XX} + \varphi_{YY} = 0. \tag{59}$$

The problem of finding the inviscid flow is now reduced to solving Eq. (59) in a domain bounded by the shock and the shear layer as shown in Fig. 4. This boundary-value problem is nonlinear, for the boundary conditions and the location of the downstream edge of the shock wave depend upon the inviscid solution. An iteration procedure, starting from a reasonable first approximation to the boundary conditions, is used to find an approximate solution of this nonlinear problem. The tendency of the LaPlace equation to smooth out discontinuities gives some assurance that such an iteration will converge, though this has not been proved in the present paper.

The origin of the X–Y coordinate system is taken as the point where the downstream edge of the shock touches the shear layer. The edge of the shock wave is not precisely defined but might be taken as the locus of points where 99% of the change across the shock wave has occurred. Since

[19] J. D. Cole, Office of Scientific Research TN 54-55, GALCIT (1954).

the mean-surface approximation will be applicable[18] the shear layer will be replaced by a sink distribution on the X axis. For the initial iteration it is assumed that the downstream edge of the shock lies on the Y axis.

The iteration is started by assuming that $u'(0, Y) = 0$. The shear-layer boundary condition is approximated as

$$v^{(1)}(X, 0) = (\gamma + 1)^{\frac{1}{2}}\varphi_Y(X, 0) = -\kappa[A(X + b)]^{-\frac{1}{2}}, \quad X \geq 0, \tag{60}$$

where

$$b = \kappa^2/A(v_{20}^{(1)})^2.$$

In (60), $v_{20}^{(1)}$ is the absolute value of $v^{(1)}$ just where the downstream edge of the shock touches the shear layer, and is determined by the matching procedure above. κ and A are as defined in Eqs. (45) and (55). Thus $v'(X, 0)$ given in (60) has the proper value at the origin and at the same time as $X \to \infty$, $v'(X, 0)$ approaches the asymptotic shear-layer behavior given by Eq. (42).

The solution of the LaPlace equation for the first iteration, is obtained by reflecting the sink distribution in the Y axis and is given by the integrals

$$\begin{aligned} v_a^{(1)}(X, Y) &= -\frac{\kappa}{\pi A^{\frac{1}{2}}} \cdot \int_{-\infty}^{\infty} \frac{Y}{(b + \xi \operatorname{sgn} \xi)[(X - \xi)^2 + Y^2]}\, d\xi, \\ u_a'(X, Y) &= -\frac{\kappa}{\pi A^{\frac{1}{2}}(\gamma + 1)^{\frac{1}{2}}} \cdot \int_{-\infty}^{\infty} \frac{(X - \xi)}{(b + \xi \operatorname{sgn} \xi)[(X - \xi)^2 + Y^2]}\, d\xi, \end{aligned} \tag{61}$$

where the subscript a refers to the first iteration with $u' = 0$ at the shock. The integrals may be evaluated in closed form,[15] and yield the important result that

$$\begin{aligned} &\text{as } Y \to \infty, \quad v_a^{(1)}(0, Y)/v_{20}^{(1)} \sim -(2b/Y)^{\frac{1}{2}}; \\ &\text{as } X \to \infty, \quad u_a'(X, 0)/v_{20}^{(1)} \sim -[b/(\gamma + 1)X]^{\frac{1}{2}}, \end{aligned} \tag{62}$$

which coincides with the asymptotic behavior of Hartunian's solution.[5]

Adams[20] has shown that changes in $u'(0, Y)$ will be of higher order when disturbances to a uniform flow are small and restricted to the region downstream of the shock; and this result was used by Hartunian. Adams' conclusion does not hold when the flow is transonic as is the case here; consequently, the second iteration must correct for the fact that $u'(0, Y)$ is in reality not negligible. With $v_a^{(1)}(0, Y)$ known from the first iteration a value of $u'(0, Y)$ which will be used in the second iteration may be determined from the Hugoniot relations across a transonic oblique shock. The fact that

$$\text{as } Y \to \infty, \; u_b'(0, Y)/v_{20}^{(1)} \sim v_{20}^{(1)}/(\gamma + 1)(Y/b), \tag{63}$$

suggests that $u_b'(0, Y)$ may be approximated by

$$u_b'(0, Y)/v_{20}^{(1)} = c_1[c_2 + (Y/b)]^{-1}, \quad Y \geq 0, \tag{64}$$

where

$$\begin{aligned} c_1 &= v_{20}^{(1)}(\gamma + 1)^{-1}, \\ c_2 &= (v_{20}^{(1)})^2/(\gamma + 1)u_{20}^{(1)}, \\ u_{20}^{(1)} &= u_b'(0, 0). \end{aligned}$$

This approximation behaves as (63) for large Y and gives the proper value of $u_b'(0, Y)$ at the origin $Y = 0$. The subscript b denotes the second iteration.

The Y axis is now replaced by a source distribution which is reflected about the X axis. In this way $v_b'(X, 0) = 0$ so that boundary condition (60) is conserved. The correction due to the fact that $u'(0, Y) \neq 0$ is thus given by the integrals

$$\begin{aligned} u_b'(X, Y) &= \frac{c_1}{\pi} \cdot \int_{-\infty}^{\infty} \frac{X}{[c_2 + (\eta/b) \operatorname{sgn} \eta][X^2 + (Y - \eta)^2]}\, d\eta \\ v_b'(X, Y) &= \frac{c_1(\gamma + 1)^{\frac{1}{2}}}{\pi} \cdot \int_{-\infty}^{\infty} \frac{(Y - \eta)}{[c_2 + (\eta/b) \operatorname{sgn} \eta][X^2 + (Y - \eta)^2]}\, d\eta. \end{aligned} \tag{65}$$

These integrals also may be found in closed form, and the resultant solution for the second iteration has the following asymptotic behavior:

$$\begin{aligned} &\text{as } Y \to \infty, \; \frac{v_b^{(1)}(0, Y)}{v_{20}^{(1)}} \sim \frac{2c_1(\gamma + 1)^{\frac{1}{2}}}{\pi(Y/b)} \ln\left(\frac{Y}{bc_2}\right); \\ &\text{as } X \to \infty, \; \frac{u_b'(X, 0)}{v_{20}^{(1)}} \sim \frac{2c_1 b}{\pi X} \ln\left(\frac{X}{bc_2}\right). \end{aligned} \tag{66}$$

Thus since $v_b'(0, X)$ and $u_b'(X, 0)$ vanish faster than $v_a^{(1)}(0, Y)$ and $u_a^{(1)}(0, Y)$, the conclusion that the inviscid solution approaches Hartunian's solution as $X, Y \to \infty$ still holds.

[20] M. C. Adams, J. Aeronaut. Sci. 16, 685 (1949).

The inviscid flow between the shock and the shear layer now will be approximated by

$$v^{(1)}(0, Y) = v_a^{(1)}(0, Y) + v_b^{(1)}(0, Y),$$
$$u'(X, 0) = u_a'(X, 0) + u_b'(X, 0). \tag{67}$$

Further corrections to the inviscid solution could be calculated; however, because of the many approximations which have already been made, further refinement is not worthwhile. Indications are that these corrections will in any case be small.

With $v^{(1)}(0, Y)$ and $u'(0, Y)$ known, the free-stream shock shape can be determined. To gain a picture of the behavior of the approximate solution above, the shock shape, $v^{(1)}(0, y)$ and $u'(x, 0)$ have been calculated using the properties of nitrogen. Figure 5 shows the shock as determined from the approximate analysis above, and u' and $v^{(1)}$ as well as Hartunian's solution are shown in Fig. 6.

In principle, the approximate analysis is similar to that employed by Hartunian; however, by introducing the concept of the shear layer and approximately accounting for the interaction between this layer and the free-stream shock, the main difficulties of Hartunian's solution have been eliminated. At the base of the shock, in the present case, velocities remain finite and the shock wave retains a finite angle instead of being tangent to the wall.

Because of the method of approximation, certain inconsistencies do remain. At the origin the derivatives of $u'(X, 0)$ and $v^{(1)}(0, Y)$ are singular so that the shock curvature is infinite even though the shock angle is finite. Clearly this is in violation of the curvature condition (53) developed in Sec. IV above; however, this singular behavior is restricted to a very small region. It has no physical significance and results from the approximate method of expressing the boundary conditions of the inviscid flow. The present analysis though providing an over-all view of the leading-edge interaction does not show the exact nature of the non-Hugoniot region at the base of the shock wave.

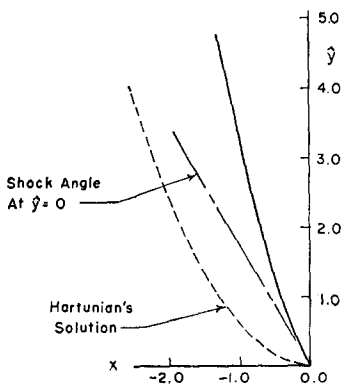

FIG. 5. Shape of the shock centerline as obtained from the approximate solution of the leading-edge interaction. (Properties of N_2 were used.)

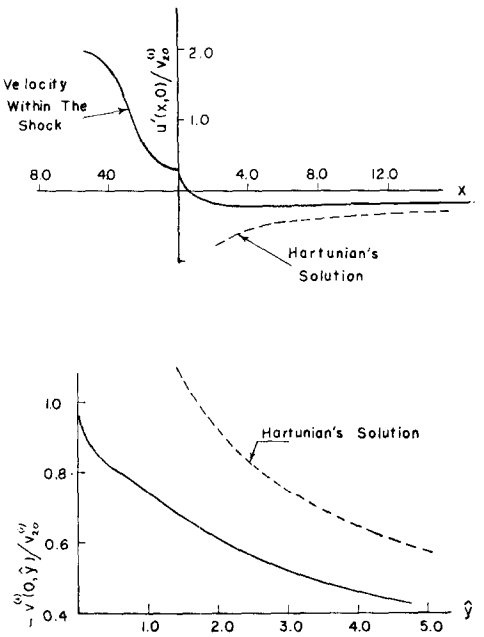

FIG. 6. The variation of u' within the shock wave and at the edge of the shear layer, and the variation of $v^{(1)}$ at the downstream edge of the shock wave. (Properties of N_2 were used.)

An interesting feature of the interaction which may be observed from Fig. 6 is that $u'(X, 0)$ overshoots the downstream Hugoniot value $u' = 0$ of the free-stream normal shock. This overshoot occurs because the shear layer sucks fluid out of the downstream flow.

VI. CONCLUSIONS

The singularity at the leading edge of a shock-induced boundary layer may be eliminated by considering the detailed interaction between the free-stream shock structure and the shear layer at the wall. By dividing the flow into a shear layer near the wall and a free-stream or shock region, it was possible to develop an approximate solution for the transition from the undisturbed flow upstream of the shock wave to the fully developed downstream boundary layer. The study of the leading edge shows that near the wall the shock structure must be two dimensional, i.e., there is a region of non-Hugoniot flow.

A key result of the analysis above is that four or five shock thicknesses away from the leading edge the approximate solution and Hartunian's solution become almost indistinguishable. Thus the effect of the singularity in Hartunian's solution appears to be confined to the vicinity of the leading edge.

Experimental verification of the theory developed above is not presently available. The results of Duff and Young[3] are not applicable. Their shock-shape measurements were made with argon in a cylindrical shock tube for Mach numbers between 1.83 and 6.33, whereas the present analysis is for two-dimensional flow and will be valid only for Mach numbers less than approximately 1.2. Further, Duff and Young's measurements do not provide details of the shock shape close to the wall.

ACKNOWLEDGMENTS

The author would like to thank Professor L. Crocco who suggested the present problem and whose comments and suggestions made the completion of this work possible.

The work described above was completed while the author was at the Gas Dynamics Laboratory at Princeton University, and was sponsored by the Air Force Office of Scientific Research under Contract AF 49(638)-465.